

Modelling Chemical Reaction in a Scalar Mixing Layer

B.L. Sawford

Department of Mechanical Engineering
 Monash University, Clayton, VIC, 3800 AUSTRALIA

Abstract

Statistics of passive and reactive scalar concentration in a scalar mixing layer are modelled using a Lagrangian particle model coupled to a micro-mixing model and using conserved scalar theory for the chemistry. Good agreement is obtained with laboratory experiments for passive scalar statistics. Reasonable agreement is obtained with laboratory data for reactive scalars on the edges of the mixing layer, but both the mean and variance are over-estimated in the middle of the layer. It is suggested that this discrepancy may be due to a flow instability in the experiments.

Introduction

Modelling chemical reactions in turbulence is well-established in chemical engineering flows such as flames and other combustion devices, but is less advanced in environmental flows. The critical aspect of the problem is that the mean rate of reaction depends on the mean of the product of the instantaneous concentrations of the reactants, not on the product of the mean concentrations. Since both turbulent mixing and chemical reaction can affect this mean product, it is important to include both of these processes, and their interaction, in the model.

When a step change in temperature in a direction transverse to the flow is acted upon by turbulence, the interface between hot and cold fluid, which thickens with distance downstream, is known as a thermal mixing layer. More generally, when the transported scalar quantity is the concentration of some contaminant species, the interface is known as a scalar mixing layer. If the temperature difference is small, or the species dilute, the scalar material has no effect on the flow and the interface is known as a passive scalar mixing layer.

The scalar mixing layer has been studied experimentally in grid turbulence using both temperature [1] (and references therein) and chemical species [2]. Bilger et al. [2] also studied the reaction of two species introduced as separated streams upstream of the grid (see their figure 1 for a schematic of the configuration). Recently de Bruyn Kops et al. [3] studied reacting scalar mixing layers using direct numerical simulation.

The reacting scalar mixing layer is an important prototype for more complex and realistic configurations. On one hand, its simplicity and symmetry make it relatively easy to study. On the other hand it increases in scale with distance from the source, and is similar in this respect to plumes from localised sources which figure so prominently in atmospheric and other environmental applications. In this paper we use a Lagrangian model for the motion of fluid particles coupled to a simple micro-mixing model to represent the turbulent transport and mixing of a passive conserved scalar in a scalar mixing layer. We then use conserved scalar theory [2] in various limits to model the statistics of chemically reactive species.

Transport and Mixing of a Conserved Scalar

In common with most theoretical approaches, for convenience we represent both the scalar mixing layer and the grid turbulence as non-stationary, spatially homogeneous analogues of the experimental systems which are stationary and inhomogeneous in

the stream-wise direction. This is achieved through the Taylor transformation $x - x_0 = x' = Ut$ and requires that the stream-wise velocity fluctuations be small compared with the mean velocity U . For generality we allow the origin of the mixing layer $x_0 = Ut_0$ to be non-zero. We thus represent the source of the conserved scalar as an instantaneous function of the cross-stream position z

$$S(z, t) = c_0(1 - H(z))\delta(t) \quad (1)$$

where $H(z)$ is the Heaviside function and we have taken the source concentration in the lower stream to be c_0 . The scalar concentration statistics are thus functions of z , t and the travel time from the grid to the source, t_0 . Note that the time origin is the source release time.

Lagrangian theory relates the 1-point displacement statistics for independent marked fluid particles to the mean concentration of the scalar field [4]. Marked particles conserve the concentration assigned to them at the labeling time, which is usually associated with the source. Much success in modelling the mean concentration under a wide range of turbulence and scalar source conditions has been obtained using stochastic models in which the velocity \mathbf{u} and position \mathbf{x} along the trajectory of a marked fluid particle are treated as a joint continuous Markov process. For decaying grid turbulence we have

$$dw = -\frac{C_0 \varepsilon}{2\sigma_w^2} w dt + \frac{w}{2\sigma_w^2} \frac{\partial \sigma_w^2}{\partial t} + \sqrt{C_0 \varepsilon} d\xi \quad (2)$$

$$dz = w dt$$

where the deterministic terms ensure that the probability density function (pdf) for the Eulerian velocity component w is Gaussian with variance $\sigma_w^2(t)$, C_0 is the Lagrangian velocity structure function inertial sub-range constant [5], $\varepsilon(t)$ is the rate of dissipation of turbulence kinetic energy and ξ is the Wiener process [6]. We represent σ_w^2 and ε as power-law functions of travel time from the grid and take $C_0 = 3$ [7].

Marked particle statistics generated using Eq. (2) produce concentration fluctuations because particles arriving at the receptor point in different realizations can have different concentrations according to their location with respect to the source at the labeling time. In order to account for the dissipation of scalar variance, we add to (2) an equation describing the evolution of the scalar concentration c along a trajectory. This is known as a micro-mixing model, and here we use the interaction by exchange with the conditional mean (IECM) model [8] for which

$$dc/dt = -(c - \langle c | w \rangle)/t_m \quad (3)$$

where $\langle c | w \rangle$ is the conditional mean concentration given the velocity and t_m is the mixing time scale. This is perhaps the simplest mixing model to satisfy the ideal properties set down by Pope [9]. In particular it ensures that the mean concentration, and other 1-point statistics such as the flux and the conditional mean concentration, are unaffected by mixing and so can be calculated from marked particle statistics. Then, we have [10]

$$\bar{c}(z, t) = \frac{1}{2} c_0 \left[1 - \operatorname{erf} \left(\frac{z}{\sqrt{2} \sigma_z} \right) \right] \quad (4)$$

and

$$\langle c | w \rangle = \frac{1}{2} c_0 \left[1 - \operatorname{erf} \left(\frac{z - \rho_{wz} w \sigma_z / \sigma_w}{\sqrt{2} \sigma_z (1 - \rho_{wz}^2)^{1/2}} \right) \right] \quad (5)$$

where $\sigma_z(t)$ is the dispersion of marked particles and the correlation between the velocity and position along a trajectory is $\rho_{wz} = (\partial \sigma_w^2 / \partial t) / (2 \sigma_w \sigma_z)$. For decaying grid turbulence Anand and Pope [11] give an analytical result for $\sigma_z(t)$. Although we do not show it explicitly, all these quantities also depend on the source time t_0 .

The mixing model (3) implies a closure for the mean scalar dissipation conditional on the scalar concentration [10]

$$\langle \varepsilon_c | c \rangle = \kappa \langle \partial^2 c / \partial x_i^2 | c \rangle = -(c - \bar{c}) / t_m \quad (6)$$

where $\bar{c}(c) = \int \langle c | w \rangle P(w | c) dw$. Note that for simplicity we use the same notation for the physical variables c and w and their corresponding sample space variables.

Various researchers have recently shown that for developing scalar fields such as plumes from small sources, the mixing time scale grows linearly with time [7, 10]. We expect the scalar mixing layer to behave similarly since its thickness grows at the same rate as a line plume. Thus we take $t_m = bt$ and determine the value of the constant b by fitting appropriate experimental data. For this purpose we use the most completely documented set of experimental results, those of Ma and Warhaft [1].

Thus we have finally a closed set of equations which can be solved for the velocity, position and concentration along a fluid trajectory. We used 5×10^5 trajectories with initial positions (at $t = 0$) distributed uniformly across the domain, initial velocities drawn from a Gaussian distribution with variance $\sigma_w^2(0)$ and initial concentrations given by the source function (1). The computational domain spanned the region $|z| \leq 0.2$ m, the width of the wind tunnel of Ma and Warhaft [1], with perfect reflection at the boundaries. Because the integration was stopped well before the width of the mixing layer (i.e. σ_z) reached the width of the domain, the results are insensitive to the boundary conditions. At specified sampling times, the cross-stream position z , the concentration c and the velocity w were sorted jointly into bins of width $0.2\sigma_z$, $0.0125c_0$ and $0.2\sigma_w$ respectively, so that joint statistics of velocity and concentration could readily be calculated as functions of cross-stream location and travel time. The mean wind speed and the turbulence decay power laws were taken from Table I of Ma and Warhaft [1].

Ma and Warhaft [1] introduced the initial step profile into the turbulence at the grid using an upstream ‘‘toaster’’ and at a range of distances down stream from the grid using a ‘‘mandoline’’. When scaled by the width of the mixing layer all their data for the mean concentration profile collapse onto the error function profile (4). Figure 1 shows that the evolution of the root-mean-square (rms) concentration fluctuations σ_c on the centreline can be represented well if we choose a value $b = 0.5$ for the constant of proportionality in the mixing time scale. This is lower than the value of 1.2 used by Sawford [7] to fit wind tunnel data for a line plume. The model with $b = 0.5$ also represents very well profiles for the rms concentration (figure 2) and, although we do not show results here, for the skewness and kurtosis of concentration fluctuations across the mixing layer.

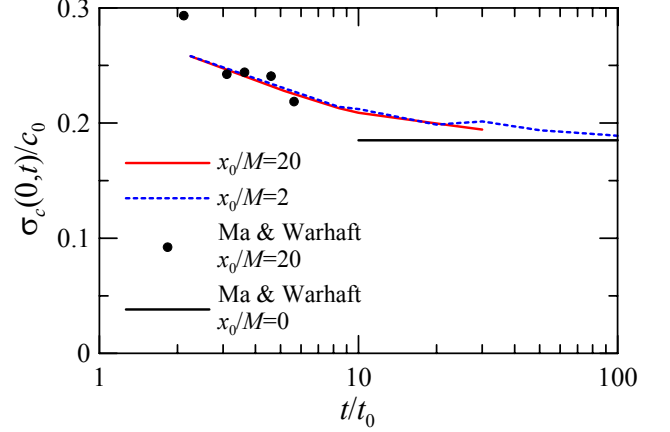


Figure 1. Comparison of model prediction for the centreline standard deviation of concentration fluctuations with the results of Ma and Warhaft [1] using a mixing time scale $t_m = 0.5t$.

The model results in figure 1 show that scaling in terms of t_0 collapses results for different source locations, and that for large values of t/t_0 the centreline rms is constant, as is also observed in the data. Thus, although we cannot explicitly model the case where the source is at the grid because the power-law representations of the turbulence diverge at the grid, we can approximate it by choosing x_0 suitably small, so that at the distance of interest $(x-x_0)/x_0$ is larger than about 50. This limit is of interest for the chemically reacting case, because $x_0 = 0$ for the experimental results of Bilger et al. [2].

We calculated the pdf for the scalar concentration $P(c)$ and the conditional scalar dissipation at a range of values of t/t_0 . Details are given in Sawford [10]. For t/t_0 greater than about two the results are well-fitted by the simple forms

$$\langle \varepsilon_c | c \rangle t_m / c_0^2 = A c^2 (1 - c)^2 \quad (7)$$

and

$$P(c) = B(\gamma) c^\gamma (1 - c)^\gamma \quad (8)$$

In the limit $t/t_0 \rightarrow \infty$, we found $A = 0.4$, $\gamma = 2$ and $B(2) = 30$. Integrating (7) over the pdf (8), substituting these limiting values and using the fitted time scale constant $b = 0.5$, we obtain the unconditional scalar dissipation

$$\langle \varepsilon_c \rangle / c_0^2 = 0.038 t^{-1} \quad (9)$$

The coefficient 0.038 may be compared with the value of 0.06 inferred by Bilger [12] from the data of Ma and Warhaft [1].

Conserved Scalar Theory for Chemistry

Consider the second-order reaction



Then the chemical source terms for species A , B and P are

$$w_A = w_B = -w_P = -k c_A c_B \quad (11)$$

where k is the reaction rate constant. Thus the quantity $c_A - c_B$ is unaffected by reaction and is known as a conserved scalar, and its statistics are identical with those already discussed. Other conserved scalars can be defined for the system (10), but they are all essentially equivalent.

Now if species A is introduced in the upper stream (stream 1) with concentration $c_{A,1}$ and species B is introduced in the lower stream with concentration $c_{B,2}$ (as in [2]), then we can define the mixture fraction F for the conserved scalar by

$$F = (c_A - c_B + c_{B,2}) / (c_{A,1} + c_{B,2}) \quad (12)$$

with the boundary conditions $F = 0$ in the lower stream and $F = 1$ in the upper stream. Thus, $1 - F$ is equivalent to the normalised scalar concentration c/c_0 in the Ma and Warhaft experiments [1].

We see from figure 2 that the conserved scalar results for the rms fluctuations are significantly lower than the model predictions and the thermal mixing layer results of Ma and Warhaft [1]. Li et al. [13] noted that this is at least partly due to an instability in the flow and by removing the instability they obtained improved agreement. Nevertheless, the reactive scalar results of Bilger et al. [2] have been affected by what is effectively excess mixing in the middle of the mixing layer.

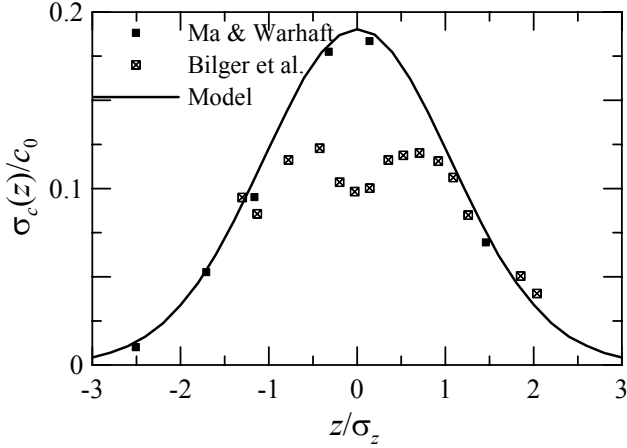


Figure 2. Comparison of model predictions for the cross-wind profile of rms concentration fluctuations with the conserved scalar results of Bilger et al. [2] at $x'/M = 21$ and the passive scalar results of Ma & Warhaft [1] for $x_0 = 0$.

The conserved scalar concept is useful because in various limits and approximations the reactant concentrations c_A and c_B , and the product concentration c_P , can be written as functions of the mixture fraction. Thus in the limit of very slow reactions, the so-called frozen limit, the reactants are unaffected by chemistry, so we have

$$c_A^f = Fc_{A,1}; \quad c_B^f = (1 - F)c_{B,2}; \quad c_P^f = 0 \quad (13)$$

At the other extreme of very fast chemistry, reaction is so fast that species A and B cannot coexist, so from (12)

$$\begin{aligned} c_A^e &= c_{A,1}(F - F_s)H(F - F_s)/(1 - F_s) \\ c_B^e &= c_{B,2}(F_s - F)H(F_s - F)/F_s \end{aligned} \quad (14)$$

where the stoichiometric mixture fraction $F_s = c_{B,2}/(c_{A,1} + c_{B,2})$ is obtained by setting $c_A = c_B$ in (12).

Another useful approximation is the so-called reaction-dominated limit, which assumes instantaneous mixing at the source followed by reaction for the travel time t from the source [2]. For $F \neq F_s$

$$\begin{aligned} \frac{c_A^{rd}}{c_{A,1}} &= \frac{F(F_s - F)}{F_s(1 - F)\exp\{(F_s - F)N_D x'/M\} - F(1 - F_s)} \\ \frac{c_B^{rd}}{c_{B,2}} &= \frac{(F_s - F)}{F_s} + \frac{(1 - F_s)c_A^{rd}}{F_s c_{A,1}} \end{aligned} \quad (15)$$

and for $F = F_s$

$$\begin{aligned} \frac{c_A^{rd}}{c_{A,1}} &= \frac{F_s}{1 + F_s(1 - F_s)N_D x'/M} \\ \frac{c_B^{rd}}{c_{B,2}} &= \frac{(1 - F_s)}{1 + F_s(1 - F_s)N_D x'/M} \end{aligned} \quad (16)$$

where the Damkohler number $N_D = k(c_{A,1} + c_{B,2})M/U$ and M is the grid mesh length.

Finally, Klimenko [14] and independently Bilger [12] have developed the conditional moment closure (CMC) theory for the mean concentration of the reactive species conditional on the conserved scalar mixture fraction, $\hat{Q}(F) = \langle c_A | F \rangle$ for example.

Bilger [12] shows that for the reacting mixing layer the CMC equation can be approximated by

$$\frac{\partial Q}{\partial \zeta} = -Q(Q - F + F_s) + \langle \varepsilon_F | F \rangle \frac{\partial^2 Q}{\partial F^2} \quad (17)$$

where $Q = \hat{Q}/(c_{A,1} + c_{B,2})$ and $\zeta = N_D x'/M$. Bilger [12] modelled the conditional dissipation in (17) as $\langle \varepsilon_F | F \rangle = \langle \varepsilon_F \rangle = 0.03t^{-1}$, which is close to (9). We solved for Q as a function of ζ and F using the conditional scalar dissipation (7) and also, for comparison, its unconditional approximation (9). We represented the numerical results for Q analytically by fitting to them the RDL formulae (16) and (17) with a retarded reaction progress variable $\zeta'(\zeta)$. For $\langle \varepsilon_F | F \rangle = 0$, the CMC approximation reduces to the reaction-dominated limit.

Now using (13) - (17) we are able to calculate the reactant concentrations (or in the case of CMC, the conditional mean concentration) along a trajectory from the conserved scalar concentration, and can then calculate statistics of these reactant concentrations as a function of cross-stream location and travel time simply by averaging over trajectories.

Results for reactive scalar statistics

In figure 3 we compare model predictions for the mean reactant concentration with the results of Bilger et al. [2] for $F_s = 0.5$, $N_D = 0.42$ (corrected by a factor of $\sqrt{2}$ after Li et al. [13]) and $Ut/M = 21$. Note that reaction depletes the mean concentration more strongly in the low-concentration side of the mixing layer; i.e. in the lower layer for species A and the upper layer for B , so the profiles as a whole are shifted towards the high concentration side. There is also a greater differentiation between the different limits and models on the low-concentration side. As noted by Bilger et al. [2], the mean concentration tends to be closer to the equilibrium limit than the frozen limit. We see that on the edges of the mixing layer the CMC calculation is in excellent agreement with the experimental results, but in the middle of the layer the experimental results lie close to the equilibrium limit.

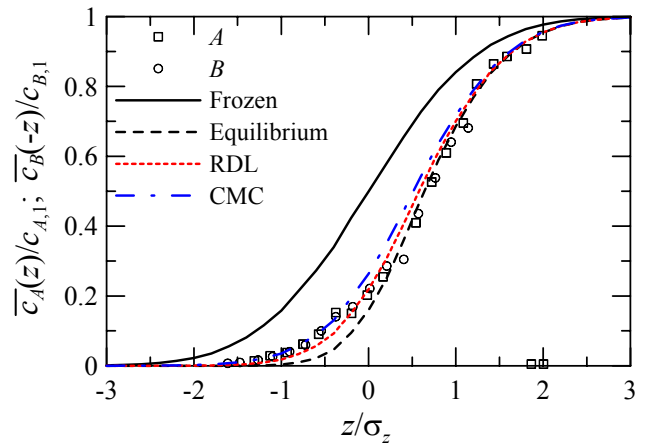


Figure 3. Comparison of model mean reactant concentrations as a function of position across the plume with experimental results [2] for $F_s = 0.5$, $N_D = 0.42$ and $Ut/M = 21$. Note that the plot for species B has been inverted in space.

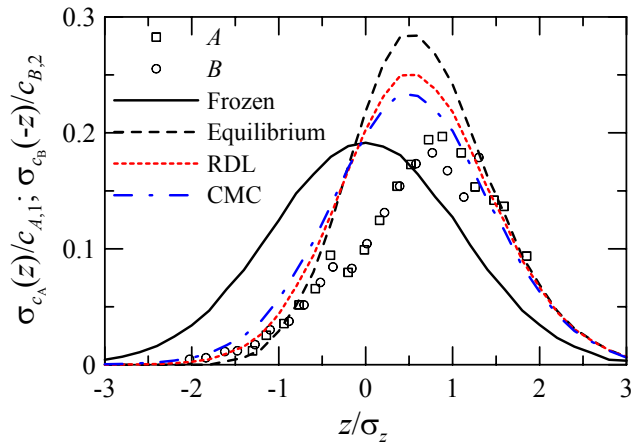


Figure 4. Comparison of model rms reactant concentrations as a function of position across the plume with experimental results [2] for $F_s = 0.5$, $N_D = 0.42$ and $Ut/M = 21$. Note that the plot for species B has been inverted in space.

The asymmetry about the centreline due to chemical reaction is even more obvious for rms fluctuations in reactant concentration as shown in figure 4, where the peak is clearly shifted towards the high-concentration side. Notice also that reaction reduces the fluctuations on the low-concentration side and increases them on the high-concentration side, as reflected by the trend from the frozen to the equilibrium results. Again the CMC model is in reasonable agreement at the edges of the mixing layer, but the experimental values are clearly lower than any of the theoretical estimates in the middle of the layer.

The discrepancy between the experimental results and the model predictions may be due to the effects of the flow instability reported by Li et al. [13]. The increased mixing due to this instability would tend to reduce the mean reactant concentration because the reactants are brought into closer contact. It would also have a direct effect in reducing fluctuations in the reactant concentrations.

For the case studied here, the CMC results using (7) and (9) are virtually indistinguishable and have not been plotted separately. This is not surprising because the unconditional value is within 30% of the conditional value for $0.25 < F < 0.75$, and values of the mixture fraction outside this range are rare, as shown by the pdf (8).

Conclusions

We have used a Lagrangian stochastic trajectory model coupled with the IECM mixing model to calculate concentration statistics in a scalar mixing layer in decaying grid turbulence. We obtained good agreement with the results of Ma and Warhaft using a

mixing time scale $t_m = 0.5t$. We also used conserved scalar theory in various limits and approximations to calculate reactive scalar statistics, and compared our predictions with the results of Bilger et al. [2]. As has been previously documented [13], a flow instability in these experiments caused enhanced mixing in the middle of the mixing layer (compared with the thermal mixing layer). It seems likely that this enhanced mixing causes a significant reduction in both the mean and rms reactant concentrations in the middle of the mixing layer. Under the conditions studied here ($F_s = 0.5$ and $N_D = 0.42$) the modelling results show that replacing the conditional scalar dissipation by the unconditional dissipation in the CMC theory is an excellent approximation.

References

- [1] Ma, B-K & Warhaft, Z., Some aspects of the thermal mixing layer in grid turbulence, *Phys. Fluids.*, **29**, 1986, 3114-3120.
- [2] Bilger, R.W., Saetran, L.R. & Krishnamoorthy, L.V., Reaction in a scalar mixing layer, *J. Fluid Mech.*, **233**, 1991, 211-242.
- [3] de Bruyn Kops, S., Riley, J.J. & Kosály, G., Direct numerical simulation of reacting scalar mixing layers, *Phys. Fluids*, **13**, 2001, 1450-1465.
- [4] Sawford, B.L., Turbulent relative dispersion, *Annu. Rev. Fluid Mech.*, **33**, 2001, 289-317.
- [5] Monin, A.S. & Yaglom, A.M. *Statistical Fluid Mechanics*, Vol. 2., MIT Press, 1975.
- [6] Gardiner, C.W., *Handbook of Stochastic Methods for Physics Chemistry and the Natural Sciences*, Springer, 1983.
- [7] Sawford, B.L., Micro-mixing models of scalar fluctuations for plumes in homogeneous turbulence, *Flow Turb. Combust.*, **72**, 2004, 133-160.
- [8] Pope, S.B., The vanishing effect of molecular diffusivity on turbulent dispersion: Implications for turbulent mixing and the scalar flux, *J. Fluid Mech.*, **359**, 1998, 299-312.
- [9] Pope, S.B., *Turbulent Flows*, CUP, 2000.
- [10] Sawford, B.L., Conditional scalar mixing statistics in homogeneous isotropic turbulence, *New J. Phys.*, **6**, 2004, 55.
- [11] Anand, M.S. & Pope, S.B., Diffusion behind a line source in grid turbulence, in *Turbulent Shear Flows 4*, editors L.J.S. Bradbury, F. Durst, B.E. Launder, F.W. Schmidt and J.H. Whitelaw, Springer-Verlag, 1985, 46-52.
- [12] Bilger, R.W., Conditional moment closure for turbulent reacting flow, *Phys. Fluids*, **5**, 1993, 436-444.
- [13] Li, J.D., Brown, R.J. & Bilger, R.W., Experimental study of a scalar mixing layer using passive and reactive scalars, *Proc. 11th Australasian Fluid Mechanics Conf.*, University of Tasmania, 1992, 159-162.
- [14] Klimenko, A.Y., Multicomponent diffusion of various admixtures in turbulent flow, *Fluid Dyn.*, **25**, 1990, 327-334.